African Journal of Advanced Pure and Applied Sciences (AJAPAS)
Online ISSN: 2957-644X
Volume 5, Issue 3, 2026
Page No: 403-417
Website: *https://aaasjournals.com/index.php/ajapas/index*
ISI 2025: 1.126 **SJIFactor 2024: 6.752** **معامل التأثير العربي: 1.62**

Surface Modification of Stainless Steel used for Medical Applications by Thin Film Deposition Using Microwave Plasma Enhanced Chemical Vapor Deposition

Sana M. Sbeta [1*], Omran A. Musbah [2], Elarbi O. Khalil [3]
[1] Plasma Research Laboratory, Authority of Natural Science Research and Technology, Tripoli, Libya
[2,3] Department of Materials & Metallurgical Engineering, Faculty of Engineering, University of Tripoli, Tripoli, Libya

تعديل سطح الفولاذ المقاوم للصدأ المستخدم في التطبيقات الطبية عن طريق ترسيب الأفلام الرقيقة باستخدام الترسيب الكيميائي البخاري المدعم بالبلازما المتولدة بالموجات الدقيقة

سناء سبيطة [1*]، عمران مصباح [2]، العربي خليل [3]
[1] المركز الليبي لأبحاث البلازما، الهيئة الليبية للبحث العلمي، طرابلس، ليبيا
[3،2] قسم هندسة المواد والمعادن، كلية الهندسة، جامعة طرابلس، طرابلس، ليبيا

[*]*Corresponding author: sbetasana01@gmail.com*

Received: May 30, 2026	Accepted: August 26, 2026	Published: September 14, 2026

Abstract:
Plasma Surface Modification (PSM) is an effective and an economical technique for many materials used in biomedical applications. A microwave Plasma Enhanced Chemical Vapor Deposition (PECVD) system (with 2.45 GHz frequency and 540 W power) was constructed for deposition of polymer-like thin films on 304L stainless steel and glass slide substrates using benzene and argon as precursor and carrier gas respectively. The surface properties of the deposited films such as chemical structure, wettability and morphology were characterized by Fourier-Transform Infrared spectroscopy (FTIR), Water Contact Angle (WCA) measurement and Field Emission Scanning Electron Microscopy (FESEM), respectively. Profilometry was used to determine the deposition rate. The effects of plasma deposition parameters (working pressure, deposition time and negative voltage bias) on the deposited films properties were investigated. FTIR analysis showed that the structure of the deposited thin film changed; in which the C≡C absorption bands became more prominent on decreasing the working pressure. A decrease in the absorption intensity for most of the stretch bands was recorded upon applying a negative voltage bias. All the treated samples registered reduced WCA below 90°; their hydrophilic surfaces became more wettable. The deposition time was found to have had the greatest influence on the rate of film deposition and the WCA measured. Wettability was successfully adjusted through plasma parameters, enabling the production of coatings suitable for specific medical applications, such as implants.

Keywords: Thin Film Deposition, PECVD, PSM, FTIR, Wettability.

الملخص

تعتبر تقنية التعديل السطحي بالبلازما (PSM) تقنية فعالة واقتصادية للعديد من المواد المستخدمة في التطبيقات الطبية الحيوية. في هذا البحث تم بناء منظومة للترسيب البخاري الكيميائي المدعم بالبلازما المتولدة بالموجات الدقيقة (PECVD) (بتردد 2.45 جيجا هرتز وقدرة 540 واط) لترسيب أفلام رقيقة شبيهة بالبوليمر على ركائز من الفولاذ المقاوم للصدأ (L340) وشرائح زجاجية باستخدام البنزين كغاز أولي والأرجون كغاز ناقل. تم توصيف الخصائص السطحية للأفلام المترسبة مثل التركيب الكيميائي باستخدام مقياس تحويرات فوريير للأشعة تحت الحمراء (FTIR)،

ومقاومة البلل بواسطة قياس زاوية تماس الماء (WCA)، والمورفولوجيا باستخدام المجهر الماسح الإلكتروني بانبعاث المجال (FESEM). كما تم حساب معدل الترسيب بعد تحديد سمك الفلم المترسب باستخدام جهاز البروفايلومتر. كذلك تم دراسة تأثير بارامترات الترسيب بالبلازما (مثل الضغط العملي، وزمن الترسيب، والجهد الانحيازي السالب) على خصائص الأفلام المترسبة. أظهر تحليل FTIR أن بنية الفيلم الرقيق المترسب تغيرت؛ حيث أصبحت نطاقات امتصاص C≡C أكثر بروزًا عند تقليل الضغط العملي، بالإضافة إلى تسجيل انخفاض في شدة الامتصاص لمعظم نطاقات التمدد عند تطبيق الجهد الانحيازي السالب. سجلت جميع العينات المعالجة انخفاضًا في WCA إلى أقل من 90 درجة؛ أصبحت أسطحها أكثر قابلية للبلل. كما أظهرت النتائج أن وقت الترسيب له التأثير الأكبر على معدل ترسيب الأفلام الرقيقة وقياس WCA. وبالتالي تم تعديل قابلية البلل بنجاح من خلال بارامترات البلازما، مما يتيح إنتاج طلاءات مناسبة لتطبيقات طبية محددة، مثل غرس الأعضاء.

الكلمات المفتاحية: ترسيب الأفلام الرقيقة، قابلية البلل، PECVD، PSM، FTIR .

Introduction

Surface modification includes all types of surface treatments and coatings that result in a change in the composition and the microstructure of the surface layer [1]. It is often performed to improve the biological, chemical and mechanical properties of the surface layer of materials [2]. Over the past 40 years, plasma has become a very useful method for surface modification and deposition of various materials [3]. Plasma Surface Modification (PSM) is an economical and an effective material processing technique used in the biomedical field because it offers the unique advantage of allowing surface properties and biocompatibility to be engineered selectively, while the bulk of the properties of the material remain unchanged. Changes in the chemical composition and properties of the surface layer of materials (e.g. wettability, metal adhesion, refractive index, hardness and biocompatibility) can be induced using PSM [4]. PSM can be classified into three categories: 1) removing materials from the surface such as plasma etching; 2) changing materials in the surface such as plasma treatment and 3) adding new materials on the surface such as thin film deposition [4-6]. The most commonly used method for thin film deposition is Plasma Enhanced Chemical Vapor Deposition (PECVD). The use of PECVD**,** or simply plasma polymerization**,** is increasing [7,8]**.** This is because PECVD is very efficient method to produce homogeneous organic thin films on large area substrates, such as metals, ceramics and plastics, and offers good control over the film properties [9]. Also, polymeric thin films obtained by PECVD have several advantages over films produced by conventional polymerization [10]. Moreover, PECVD is a green technology (i.e. environmentally benign) compared to other material processing methods. In addition, it can occur at moderate temperature compared to conventional chemical reaction [3]. In PECVD processes, plasma can be generated by direct current (DC), radio frequency (RF) and microwave (MW) discharges [11]. Microwave discharges are widely used for generating cold plasma at pressures from 10^{-5} Torr up to an atmospheric pressure of 760 Torr in the pulse and continuum wave regimes at incident powers ranging from several Watts to hundreds of kW for different applications [12]. Magnetrons are the most common microwave generators because of their low cost and availability in the market for domestic use**,** such as in microwave ovens [13]. Microwave-plasma polymerization is an attractive method for obtaining thin films [14]. A variety of medical devices such as artificial hip**s** and knee joints, coronary stents and heart valves are routinely implanted into the human body. These devices may come in contact with body fluids which contain about 1% NaCl; increasing the likelihood of corrosion that may have harmful effects on both the body and implants [**7**]. The ideal biomedical implants should have good mechanical properties while the surface should have good biocompatibility [4]. Many types of materials are being used in biomedical applications including metals, alloys, polymers, ceramics, composites, and glasses [4,15]. For structural applications in the body (i.e. implants), the principal metals used are titanium-based alloys, cobalt-based alloys and stainless steels [15]. The common grades of stainless steels used in this field are the Austenitic stainless steel 316 and 304. The Austenitic stainless steel 304 is widely used in many engineering applications such as in the manufacturing, nuclear, chemical, oil and petrochemical, and food industries, as well as in the medical industry for biomedical implants [16]. Stainless steel is naturally a biocompatible material. Its biocompatibility can be further improved by modification of its surface energetics. The biocompatibility of a material is determined by the interactions between the implant and biological system on the micrometer and nanometer scale, and the physicochemical surface properties such as chemical composition, wettability and surface energy play an important role. PSM has recently drawn much interest from the field of medicine and it is now used to improve the function and the longevity of biomedical materials [4]. PSM (such as plasma polymerization) of biomedical materials is becoming an increasingly popular method to improve device multi-functionality, tribological and mechanical properties, and the biocompatibility of artificial devices; and so, obviating the need to develop costly and time-consuming brand-new materials [4]. Beside the previous mentioned characterization, PSM of biomedical materials is used to clean a surface, reduce thrombogenicity and adhesion of cell and bacterial, eliminate protein adsorption and increase lubricity (by increasing the surface hydrophilicity i.e. more wettable), alter transport properties, increase hardness, and

enhance corrosion resistance [17]. Greater retention of the monomer functional group is observed in the resulting polymeric film with pulsed plasma polymerization [18]. The development of chemical and biological stability of biomedical materials against corrosive body-fluid environments is a widespread research interest [3,19-21]. In this research, a pulsed microwave PECVD system was constructed to deposit polymer-like thin films on 304L stainless steel substrates and on glass substrates for the FTIR analysis. The 304L is a low carbon variant of 304-grade stainless steel. Benzene and argon were used as precursor and carrier gas respectively. The main objectives of this research are 1) to deposit thin films on stainless steel via pulsed microwave PECVD and 2) to investigate the effects of deposition parameters (i.e. working pressure, time of deposition and negative voltage bias) on the properties of the deposited thin films. These films are characterized by Fourier Transform Infrared spectroscopy (FTIR), Water Contact Angle (WCA), Field Emission Scanning Electron Microscopy (FESEM) and Profilometer techniques.

Mechanism of Plasma Polymerization

The simple mechanism of plasma polymerization presented in Figure 1 is based on three steps: 1) reactive sites generation, 2) propagation and 3) termination [22]. The first step is generating the active sites such as free radicals by plasma to initiate the polymerization reaction process. The second step is the propagation of the chain growth with free radicals in which polymer molecules (P_i) is formed by continuous addition of monomer molecules (M), which can undergo, for example, a classic radical polymerization. The third step is the termination of free radicals. Along with other active species, free radicals dominate the ending of the chain growth [22].

Free radicals are the primary species propagating chain growth, both in the gas phase and on the surface of the

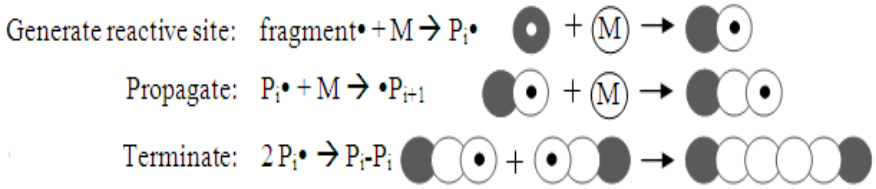

Figure 1. Simple Mechanism of Plasma Polymerization. [**22]**

deposited polymer. These species are formed in the gas phase through the collision of free electrons with monomer molecules and on the surface of the growing polymer film through the impact of ions and electrons. Surface free radicals are also produced through the adsorption of a part of the radicals formed in the gas phase. Subsequent growth of the polymer film occurs by the reaction of surface-free radicals with either gas-phase free radicals or unsaturated monomer [23].

PLASMA POLYMERIZED THIN FILM GROWTH

The growth of plasma polymers is less well understood, although the mechanisms of polymer growth have been well characterized. This is because many random processes occur in the plasma phase and the species which contribute to film growth may be neutral, radical, ionic or even metastable. The monomer undergoes fragmentation and oligomerization in the plasma phase before depositing on the substrate, and then the growing film is subjected to etching by high-energy ions. Thus, the resulting film is a highly cross-linked organic layer, which may retain some functional groups from the monomer [24]. The amount of monomer can be increased by increasing the working pressure. The polymer chain grows by addition of monomer molecules (M) and chain growth is predominately terminated by radical recombination, thus forming a polymer [26].

$$M + plasma \rightarrow fragments^{\bullet}(initiation)$$
$$fragments^{\bullet} + M \rightarrow fragment - M^{\bullet} \ldots \rightarrow fragment - M^{\bullet} + M \rightarrow P_n^{\bullet}(chain - growth)$$
$$2P_n^{\bullet} \rightarrow P_n^{\bullet} - P_n^{\bullet}(termination)$$

Figure 2 illustrates the polymerization growth mechanism with two distinct cycles involving single and divalent reactive species. The process involves a series of reactions, including additions, oligomer formation, and cross-cycle interactions, ultimately resulting in polymer deposition on the substrate [27].

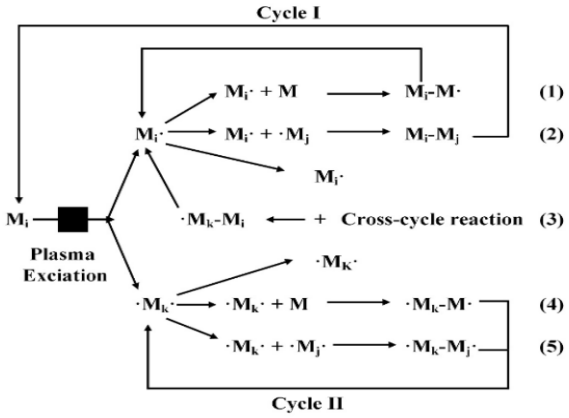

Figure 2 The schematically polymerization growth

The polymerization process is described by a two-cycle model as shown in Figure
Cycle I: Involves activation and reactions of single-site reactive species.
Cycle II: Involves reactions of divalent reactive species (likely free radicals).
The ions are considered less significant in the growth process due to charge limitations [27].

Growth Reactions:

Reactions (1, 4, 5): Addition reactions similar to initiation and propagation in chain-growth polymerization.
Reaction (2): Oligomer formation (similar to termination in chain-growth).
Reaction (3): Cross-cycle reaction between single and divalent species.
As the size of gaseous species increases, their vapor pressure decreases, leading to deposition on the substrate as a polymer.

Material and methods

Two types of substrates were used for the thin film deposition and measurements in this study: disc shaped samples with 8 mm thick and 16 mm diameter of 304L grade stainless steel (17 wt% Cr and 10 wt% Ni) and glass microscopic slides (for FTIR analysis). The surfaces of the disc samples were wet ground on silicon carbide paper down to 2000 grit and then polished with alumina. Finally, they were cleaned in an ultrasonic bath using acetone and distilled water then dried just before loading into the deposition chamber.

Plasma Deposition System and Procedure

A home-made pulsed microwave plasma system, shown schematically in Figure 3(a), was constructed for the deposition of the polymer-like thin films. The system, depicted in Figure 3(b), consists of the deposition chamber, vacuum system, and microwave generator (plasma source). The deposition chamber is composed of a stainless steel cylindrical vessel provided with four ports for vacuum system, gas inlet, wave-guide and a glass window for observing the deposition process. The vacuum system consists of a turbo-molecular pump backed by mechanical pump and pressure gauges. The microwave is generated by the commercial magnetron (microwave furnace) at frequency of 2.45 GHz with maximum power of 900 W, which is transmitted to the chamber via a waveguide. After evacuating the chamber to a base pressure of ~0.1 mTorr, thin films were deposited from benzene (C_6H6) by PECVD on 304L stainless steel and glass substrates at various deposition parameters as indicated in Table 1. Microwave plasma was generated by pulsing for 18 sec (ON state) and rest for 3 sec (OFF state), so the deposition time was the duration of pulsing multiplied by the number of pulses. Before deposition, the microwave plasma of argon gas was applied to the samples to remove any contaminations or organic oxides from the surface of samples and the chamber wall (i.e. pre-cleaning process for both samples and chamber). This process was carried out at 180 W of microwave power and working pressure of 3.7 mTorr for 15 min. The deposition process was carried out with argon as the carrier gas at (Ar/C_6H_6) mixture ratio of (30:70). By adjusting these parameters, the nature and properties of deposited thin films were varied.

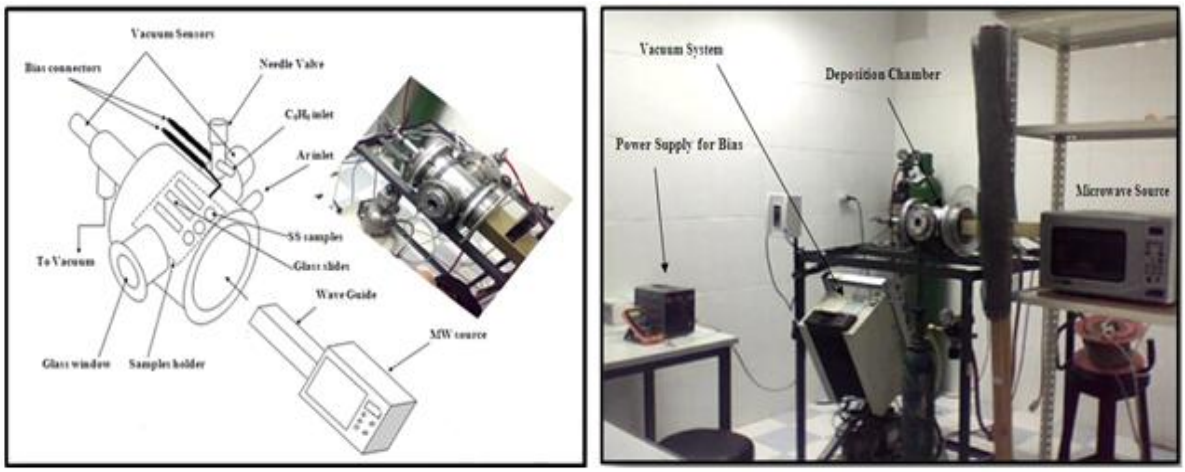

Figure 3 (a) Schematic Diagram and (**b**) Photograph of the Pulsed Microwave Plasma Deposition System.

Table 1. Parameters of the Deposition Process

Parameter	Value
Power	540 W
Base pressure	0.088 – 0.13 mTorr
Working pressure	10, 30, and 50 mTorr
Deposition time	5, 15, and 30 min
Bias voltage	-400 V
Ar/C_6H_6 ratio	30:70

The effects of the deposition parameters of working pressure, deposition time and negative voltage bias on the properties of the deposited thin films were investigated in this research.

Characterization of Plasma Polymerized Films

The deposited thin films were analyzed by the following characterization techniques; using microscopic glass slide samples for FTIR analysis and stainless steel samples for the other characterization: (1) Fourier Transform Infrared Spectroscopy (FTIR) for chemical structure and functional group identification using Thermo Scientific Nicolet iS10 FTIR Spectrometer (ATR) and OMNIC software; (2) Water Contact Angle (WCA) measurements using Theta Lite Optical Tensiometer TL100 to analyze the surface wettability (hydrophilicity/hydrophobicity); (3) Profilometer for measuring film thickness by Step Heights Method using P-6 Stylus Profiler in order to determine the deposition rate; and (4) Field Emission Scanning Electron Microscope (FESEM) and Energy-Dispersive X-ray spectroscopy (EDX) for surface morphology and elements analysis of steel sample, respectively.

Results and discussion

The untreated stainless steel sample was analyzed by Energy-Dispersive X-ray spectroscopy (EDX). The EDX spectrum of the sample shows three types of peaks (L_α, K_α and K_β), these peaks are displayed in Figure 4 and listed in Table 2.

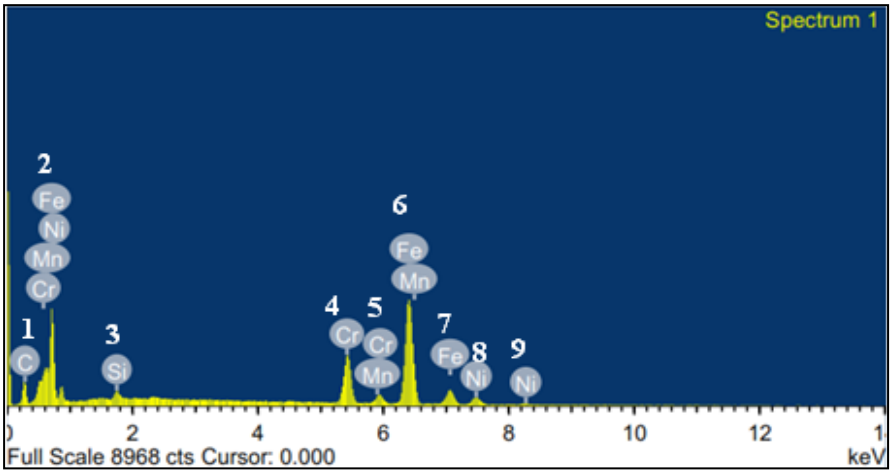

Figure 4. Energy-Dispersive X-Ray Spectrum (EDX) of Untreated Stainless Steel Sample.

Table 2. Type of Peaks Collected from Energy-Dispersive X-Ray Spectroscopy (EDX).

Element	**C**	**Fe**			**Cr**			**Mn**			**Ni**			**Si**
Peak type / Peak No	K_α	K_α	K_β	L_α	K_α	K_β	L_α	K_α	K_β	L_α	K_α	K_β	L_α	K_α
1	0.277	---	---	---	---	---	---	---	---	---	---	---	---	---
2	---	---	---	0.705	---	---	0.572	---	---	0.637	---	---	0.790	---
3	---	---	---	---	---	---	---	---	---	---	---	---	---	1.740
4	---	---	---	---	5.415	---	---	---	---	---	---	---	---	---
5	---	---	---	---	---	5.950	---	---	5.900	---	---	---	---	---
6	---	6.405	---	---	---	---	---	6.500	---	---	---	---	---	---
7	---	---	7.100	---	---	---	---	---	---	---	---	---	---	---
8	---	---	---	---	---	---	---	---	---	---	7.480	---	---	---
9	---	---	---	---	---	---	---	---	---	---	---	8.260	---	---

FTIR Analysis

The compositional changes in the molecular structure of the thin films deposited on the glass slides from benzene vapor under present experimental test conditions were observed clearly when the benzene infrared spectrum (shown in Figure 5) was compared with the other spectra of the deposited thin films (shown in Figures 6, 7, 8). The bands in the aromatic ring did not appear in the spectra of the deposited thin films which indicated a complete decomposition of benzene vapor. The bond frequency, absorption and functional groups of the thin films deposited on glass slides are illustrated in Table 3. This identification was made with the assistance of Spectroscopic Handbook on Chemistry Data [25]. The bands related to the (O-H) group with different

intensities were detected in the deposited thin films spectra. Since there was no oxygenated compound in the reacting species, the presence of these bands could be attributed to presence of some humidity in the deposition chamber. This was confirmed by analyzing the spectra of deposited thin films shown in Figure 6 after doing a pre-cleaning step and using argon as a carrier gas with (Ar/C_6H_6) ratio of 30:70. The effect of working pressure on the structure of deposited thin films at 30 min deposition time is given in Figure 7. The chemical structure changed when the working pressure was increased. For instance, the weak peaks of the carbon triple bond (C≡C) were recorded at 2177 & 2185 cm^{-1} at 10 and 30 mTorr**,** respectively**.** These peaks disappeared when the working pressure was raised to 50 mTorr. Instead**,** the hydrogenated carbon bond (C-H) was detected at 2945 cm^{-1}. This change in the nature of the chemical structure of the deposited thin films could be attributed to an increase in the amount of benzene gas entering the deposition chamber. The absorption intensity increased by increasing the deposition time as shown in Figures 8 and 9, and the films formed became thicker; though exhibited the same chemical structures (i.e. same functional groups). The FTIR analysis indicated that the deposition process in this work was more effective at 30 min deposition time. Figure 10 shows the effect of negative voltage bias (-400V) on the bond absorption of the thin film deposited at 50 mTorr for 15 min. As can be seen, a higher percentage of transmittance (i.e. lower absorption) for most of the stretch bands was recorded. This is particularly true for the (O-H) and (C=C) stretch bands. The absorption of various stretch bands showed a gradual decrease in absorption intensity from (C-H) alkanes to (O-H) group.

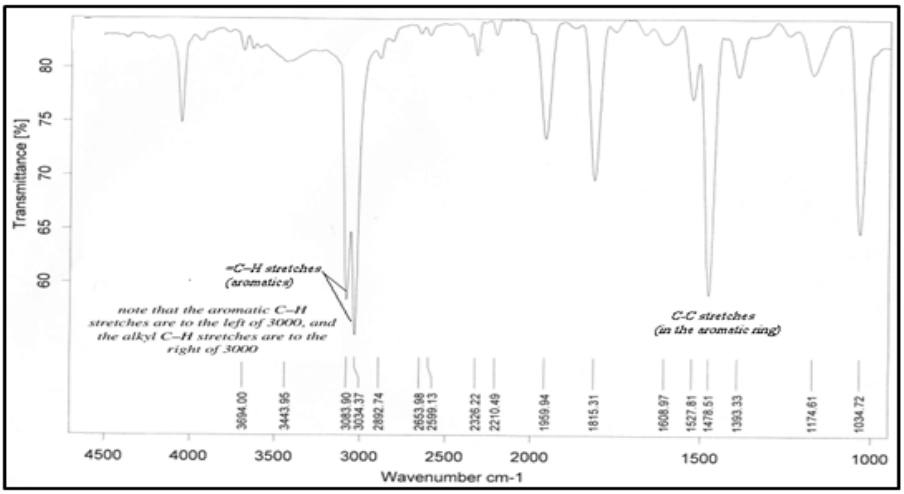

Figure 5. IR Spectrum of Benzene C_6H_6

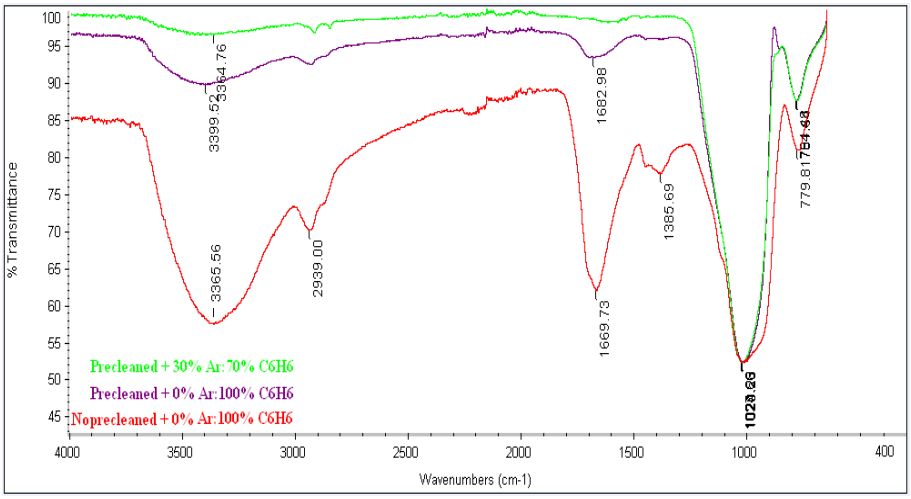

Figure 6. IR spectra of thin films deposited with/without pre-cleaning and 30%Ar:70%C_6H_6)

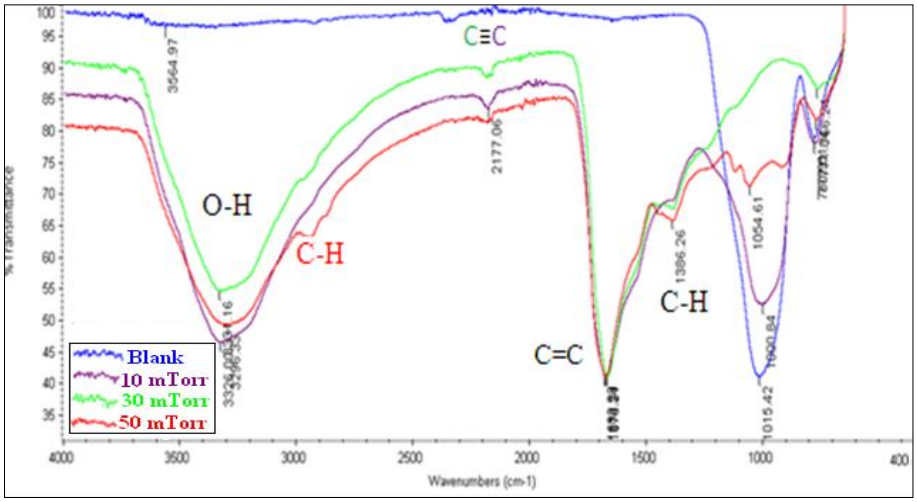

Figure 7. IR Spectra of Thin Films Deposited at 10, 30 and 50 mTorr Working Pressure for 30 min Deposition Time.

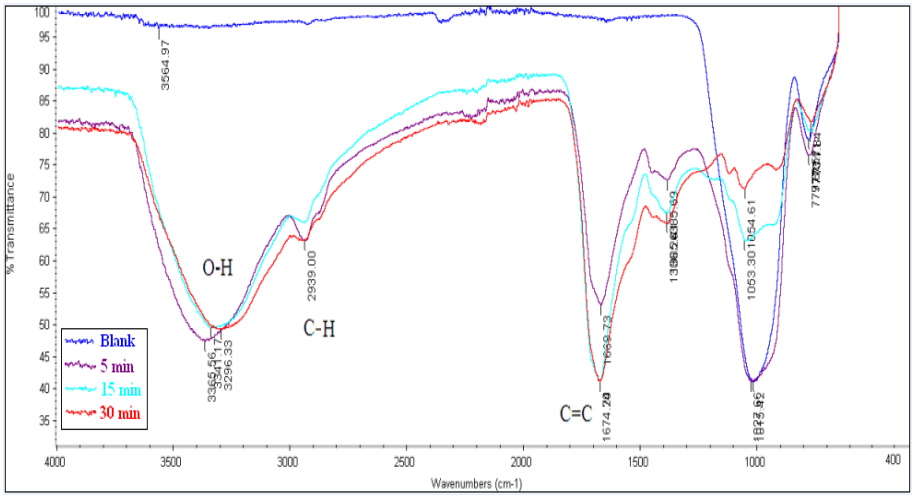

Figure 8. IR Spectra of Thin Films Deposited at 50 Torr Working Pressure

Table 3. Identification of Bond Frequency, Absorption Intensity and Functional groups of the thin films deposited on glass slides.

Bond	Wave number (cm^{-1})	Absorption intensity	Functional group
O – H str	3428 - 3296	S, br	Polymeric-alcohol
C – H str	2945 - 2939	m	Alkanes
C ≡ C str	2186 - 2177	w	Alkynes
C = C str	1683 - 1669	v	Alkenes
C – H str	1457 - 1385	m-w	Alkanes

Absorption Intensity: s: strong, w: weak, br: broad, m: medium, v: variable

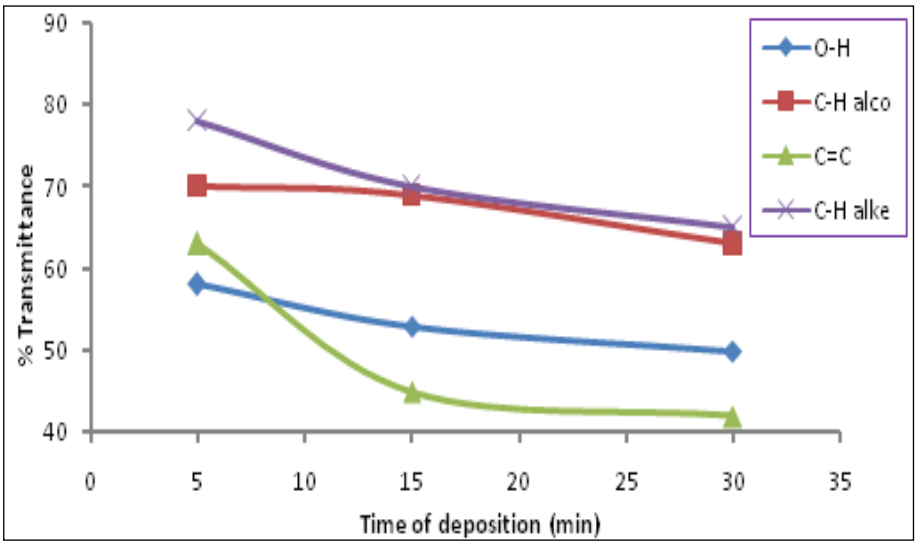

Figure 9. The Effect of Deposition Time on the Absorption Intensity of the Bonds in the IR Spectra of the Thin Films Deposited at 50 mTorr

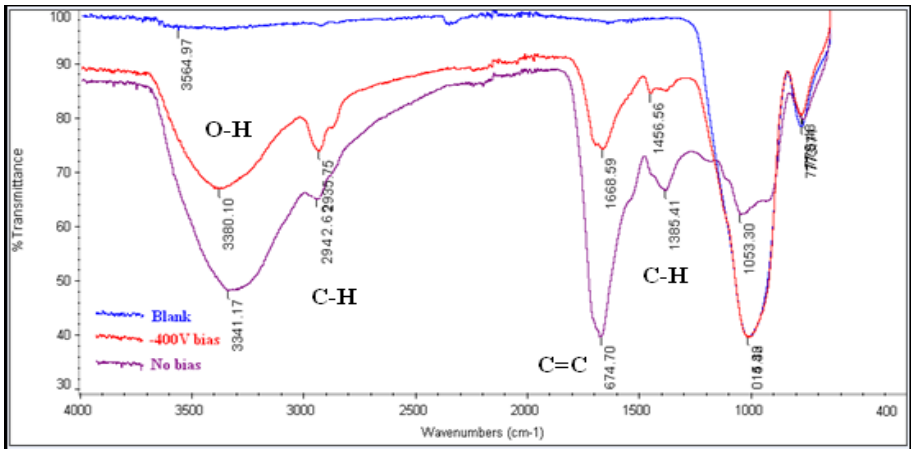

Figure 10. The Effect of Applying -400 Volt Bias on the Bond Absorption of Thin Film Deposited at 50 mTorr for 15 min.

Surface Wettability

The hydrophobicity and hydrophilicity of a solid surface is usually expressed in terms of wettability that can be quantified by contact angle measurement [26]. A lower contact angle (i.e. higher Surface Free Energy, SFE) indicates good wettability. Conversely, a higher contact angle (i.e. lower Surface Free Energy SFE) means poor wettability. The surface wettability of the deposited thin films on the 304L stainless steel (SS) substrates was analyzed by measuring the water contact angle (WCA) on the thin films deposited from benzene at different deposition parameters. As the results in Table 4 show, the contact angle (θ°) is lower than 90° for all the samples, and hence, they are classified as hydrophilic surfaces (i.e. wettable surfaces). The WCA was decreased from 81° for untreated bare 304L SS surface to 33° and 30° for the deposited thin films at working pressures of 10 and 30 mTorr, respectively. But at 50 mTorr, the treated surface still registered a decrease in the water contact angle (to 44°). As Figure 10 shows, this decrease was smaller than the others due to a change in the chemical structure of the deposited thin films as shown in the IR spectra in Figure 6. On the other hand, an increase in the time of the deposition led to a decrease in WCA and an increase in the SFE as shown in Figure 11. According to the results shown in Table 4, the deposition time seems to have a greater influence on the measured WCA and SFE when compared with the effect of working pressure.

Table 4. Results of Contact Angle and Surface Free Energy Measurements.

Parameters / Samples No	Working pressure (mTorr)	Time of deposition (min)	WCA* (θ°) [degrees]	SFE* [mN/m]	Remarks
Bare metal			81.20±0.88	35	
T1	10	30	32.61±0.56	63	Effect of working pressure
T2	30	30	29.84±0.60	65	
T3	50	30	44.35±1.10	75	
T4	50	5	71.48±1.11	46	Effect of deposition time
T5	50	15	67.18±1.31	49	
T3	50	30	44.35±1.10	57	
T5	50	15	67.18±1.31	49	No bias
T6	50	15	70.65±0.67	41	-400v bias

*SFE: Surface Free Energy *WCA: Water Contact Angle

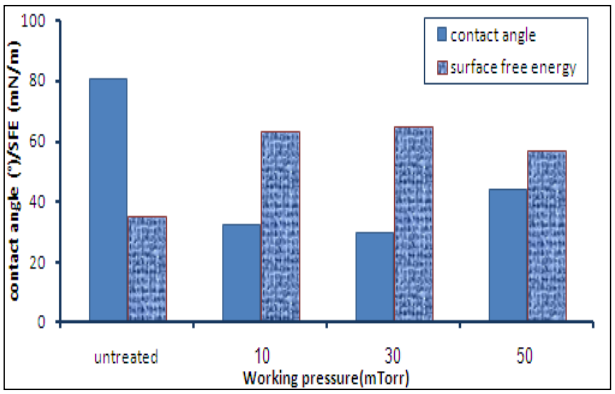

Figure 10. The Effect of Working Pressure on WCA and SFE of the Thin Films Deposited for 30 min**.**

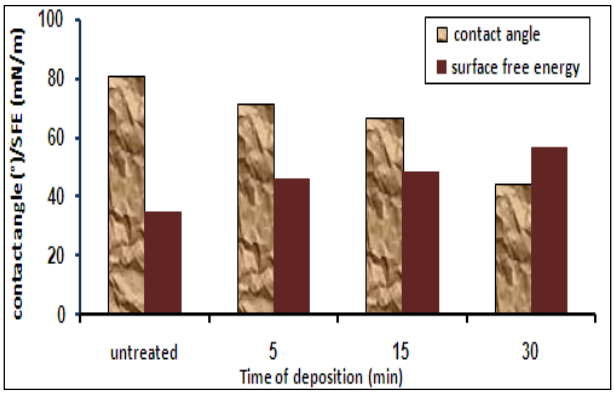

Figure 11. The Effect of Deposition Time on WCA and SFE of the Thin Films Deposited for 50 mTorr.

In order to determine the rate of plasma deposition of the hydrogenated carbon films on 304L SS substrates, a series of film thickness gauging measurements was made on a group of coated samples as given in Table 5. An investigation of the effects of deposition parameters on film deposition rate showed that the deposition time had a greater influence on the rate of film deposition compared with the effect of working pressure. For instance, the film deposition rate after 15 min is ~68% of the initial rate after 5 min deposition at constant pressure. After 30 min of deposition, the rate is only 38% of the initial rate at constant pressure of 50 mTorr. As can be seen in the table, a higher rate of film deposition was achieved at the beginning of deposition process. The highest film deposition rate of 66 Å/s was achieved with 30% Argon sputtering of test sample after the pre-cleaning step**,** which underlines the importance of surface preparation for thin film deposition.

Table 5. The Effects of Deposition Parameters on Film Deposition Rate

Parameters / Samples No	Working Pressure (mTorr)	Deposition Time (min)	Film Thickness (μm)	Deposition Rate (Å/s)	Remarks	
T1	10	30	0.616	3	Deposition rate ↑ as working pressure ↑ in the same film structure	
T2	30	30	4.672	26		
T3	50	30	4.060	23		
T4	50	5	1.718	57	Deposition rate ↓ as deposition time ↑	
T5	50	15	3.527	39		
T3	50	30	4.060	23		
T5	50	15	3.527	39	No bias	Deposition rate ↓ with bias
T6	50	15	2.42	27	-400 V bias	
T7	30	5	0.350	12	100% C_6H_6	Deposition rate ↑ with Ar
T8	30	5	1.985	66	Ar:C_6H_6 30:70	

From the results in Tables 4 and 5, it can be inferred that film wettability on coated stainless steel can be further improved by longer deposition time and lower deposition rate, as shown in Figure 12, which will create better possibility for the formation of more hydrogen bonds between water molecules and the film. However, it is not advisable to grow thin films for extended periods of time since this would lead to poor film adhesion to substrate due to the intrinsic stress caused by increasing film thickness, and it would probably have negative effects on other physical and mechanical properties as well.

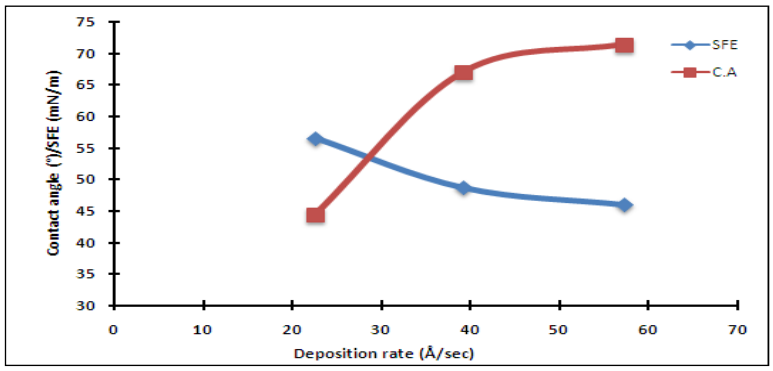

Figure 12. Contact Angle and SFE vs Deposition Rate of the Thin Film Deposited at 50 mTorr for 5, 15 and 30 min.

Visual Inspection

In this inspection, the tested samples were examined in terms of color, adhesion and uniformity of the deposited thin films by the naked eye. The change of monomer pressure (i.e. working pressure) plays an important role in the deposition process. Visual examination of the coated SS samples showed uniformly deposited films with golden yellow color at range of working pressure 10 to 50 mTorr, as exhibited in Figure 13. However, at higher working pressures 90 and 70 mTorr, poor quality deposition was evident. Flaking of the thin films deposited at 90 mTorr for 3 min and peeling off from the sample was evident, as shown in Figure 14. Good deposition of the thin films, produced at 70 mTorr at low deposition time (18 and 36 sec), with good adhesion were evident just after the deposition process, but after a few days**,** the films peeled off gradually, as exhibited in Figures 15 (a)

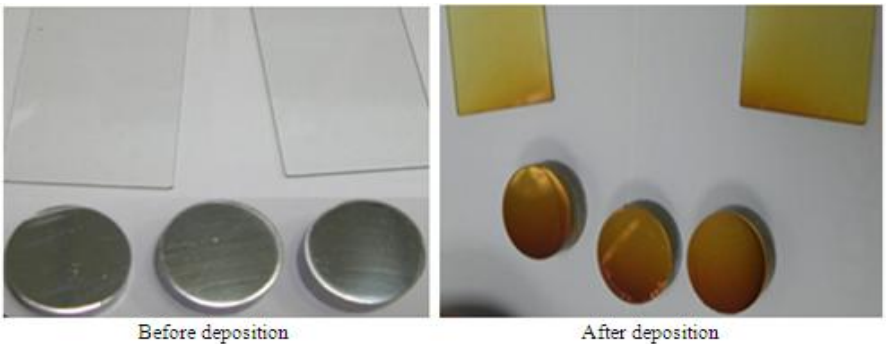

Figure 13. Golden Yellow Color of Thin Films Deposited on Stainless Steel and Glass Slides Samples.

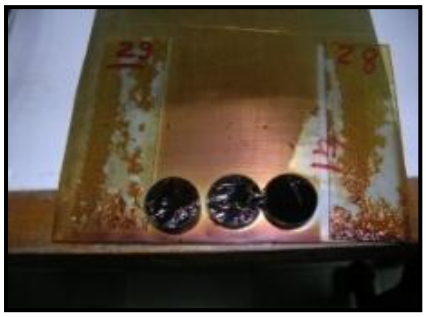

Figure 14. Thin film deposited at 90 mTorr for 3 min (poor quality deposition)

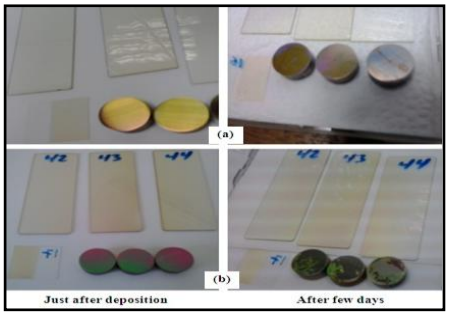

Figure 15. Thin film deposited at 70 mTorr for (a) 18 sec and (b) 36 sec.

and (b).

Surface Morphology by FESEM Analysis

Figures 16 (a, b, c) show the FESEM images of the untreated sample surface, flaking of the thin films deposited at 30 mTorr for 30 min (i.e. poor-quality deposition) and the uniform thin films deposited at 50 mTorr for 5 min (i.e. better-quality deposition). The low adhesion of the (C–H) films on stainless steel was attributed to poor chemical binding between a-C:H and metal and/or high internal stresses inside the deposited films leading to film flaking, then peeling off from the sample edge as shown in Figure 16 (b). The intrinsic stress of the films is increased by **1)** increasing the thickness of the film as evident in Figures 17 (a, b, c), 2) the nature of the film chemical structure as presented in IR spectra shown in Figure 6, and 3) the type of substrate. The problem of low adhesion can be solved by the deposition of a very thin intermediate layer between the metal surface and the (C–H) films. An amorphous hydrogenated silicon (a-Si:H) film is commonly used as an intermediate layer between metal and deposited film especially for coating of toxic substrates [7]. The effect of pre-cleaning on the surface of the sample before deposition was clearly observed. The contaminations under the thin films as shown in Figure 18 (a) were removed and so a smooth deposited thin films from only benzene were obtained as shown in Figure 18 (b). The roughness of the deposited thin films was increased by using a mixture of argon and benzene with ($Ar:C_6H_6$) ratio of (30:70) after the pre-cleaning step, as shown in Figure 18 (c).

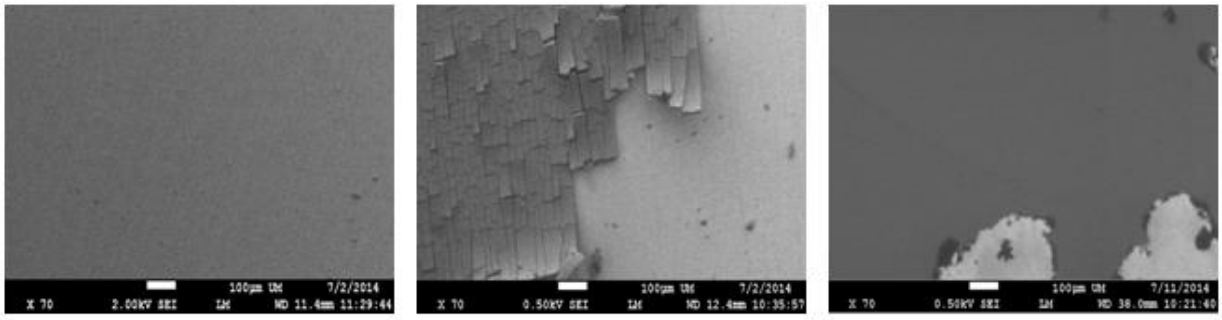

Figure 16 (a,b,c). FESEM Images of (a) Untreated Sample, (b) the Shape of Flakes Formed in Thin Film Deposition at 30 mTorr for 30 min and (c) Uniform Thin Film Deposited at 50 mTorr for 5 min (X 70).

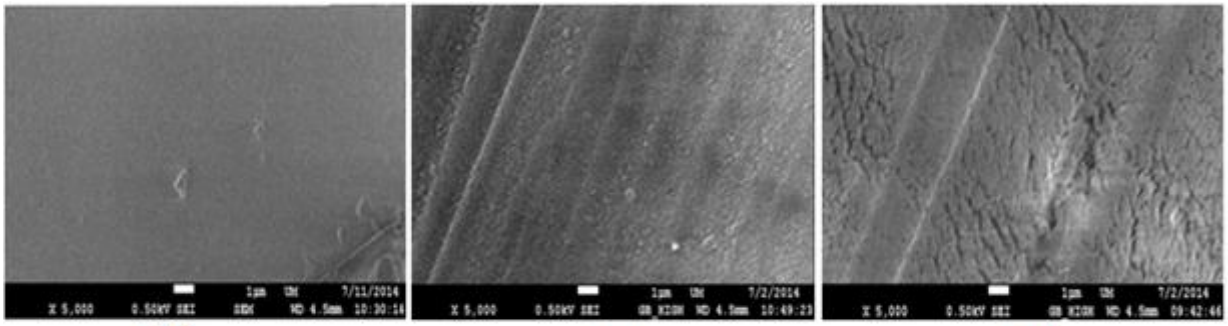

Figure 17 (a,b,c). FESEM Images of Thin Film Deposited at 50 mTorr for Deposition Time of (**a**) 5 min, (**b**) 15 min and (**c**) 30 min **(X 5,000).**

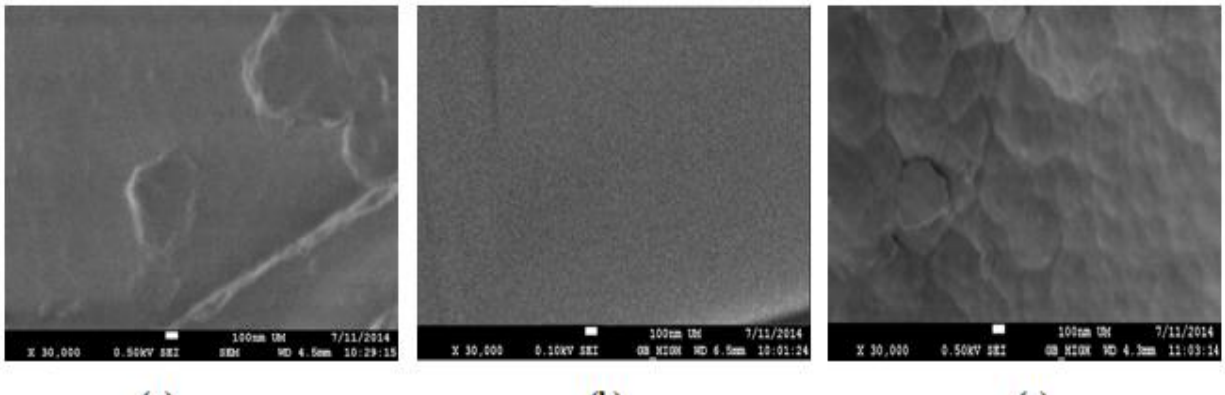

Figure 18 (a,b,c). FESEM Images of Thin Film Deposited (**a**) Without Pre-Cleaning 100% C_6H_6, (**b**) With Pre-Cleaning 100% C_6H_6 and (**c**) With Pre-cleaning 30% Ar:70% C_6H_6 (X 30,000).

Conclusion

Thin films deposited in this research were obtained from C_6H_6 and Ar-C_6H_6 mixtures decomposed in a 2.45 GHz pulsed-microwave plasma. FTIR analysis indicated the decomposition of the benzene ring and formation of a-C:H films in aliphatic group. The chemical structure of the thin films was changed by decreasing the working pressure in which the C≡C absorption bands became more prominent. At higher working pressure, the deposited films were flaking and then peeled off. The films thickness was increased by increasing the deposition time leading to an increase in the internal stress of the films which caused debonding and flaking of the films. The time of deposition was the most influential factor on the films deposition rate and films surface wettability. The highest film deposition rate of 66 Å/s on SS substrate was achieved with 30% Argon sputtering of test sample after the pre-cleaning step**,** which underlines the importance of surface preparation for thin film

deposition. All the samples had contact angle (θ) lower than 90° so they are classified as hydrophilic (i.e. wettable) surface. This work showed that wettability can be adjusted by the plasma parameters, which would enable the production of coatings with properties suitable for specific practical applications, such as in biomedical devices (e.g. implants).

Further Research

It is proposed that further research should carried out to investigates the corrosion behavior of the deposited amorphous hydrogenated carbon (a-C:H) films on 304L SS. The research would employ Electrochemical Impedance Spectroscopy (EIS) using Gamry Electrochemical Measurement System. The aim of the research is to choose the optimum plasma deposition parameters for surface modification of this grade of stainless steel that can be used for medical applications.

Acknowledgments

The authors wish to thank the Libyan Center for Plasma Research, Libyan Authority for Scientific Research for their financial support to this research; the Plasma Technology Research Center, Department of Physics, Faculty of Science, University of Malaya, Malaysia and Department of Materials and Metallurgical Engineering, Faculty of Engineering, University of Tripoli for providing the experimental facilities, without which this research would have not been possible. They also wish to extend special thanks to Dr. Abdulmagid Bouzed - the director of the Libyan Center for Plasma Research in Tripoli-Libya, Prof. Wong Chiow San & Dr. Chin Oi Hoong in Kuala Lumpur- Malaysia and Dr. Ahmed Hadoud in the UK.

Compliance with ethical standards

Disclosure of conflict of interest

The authors declare that they have no conflict of interest.

References

[1] D.M. Mattox, "Introduction", in *Handbook of Physical Vapor Deposition (PVD) Processing*, edited by D.M. Mattox, Albuquerque: William Andrew Publishing, 1998, pp. 29-55. doi: 10.1016/B978-081551422-0.50002-4.

[2] X.Y. Liu, P.K. Chu and C.X. Ding, Surface modification of titanium, titanium alloys and related materials for biomedical applications, *Mater. Sci. Eng. R Rep.*, 47, 49–121 (2004). doi: 10.1016/j.mser.2004.11.001.

[3] Z.H. Zhang, "Surface Modification by Plasma Polymerization and Application of Plasma Polymers as Biomaterials", Ph.D. Thesis, Johannes Gutenberg University Mainz, 2003, pp. 1-17.

[4] P.K. Chu. J.Y. Chen, L.P. Wang and N. Huang, Plasma-surface modification of biomaterials, *Mater. Sci. Eng. R Rep.*, 36, 143–206 (2002). doi: 10.1016/j.mser.2004.11.001.

[5] P. Favia and R. d'Agostino, Plasma treatments and plasma deposition of polymers for biomedical applications, *Surf. Coat. Tech.* 98, 1102-1106 (1998). doi: 10.1016/S0257-8972(97)00285-5.

[6] G. Szabó, L. Kovács, K. Vargha, J. Barabás and Z. Németh, A new advanced surface modification technique – titanium oxide ceramic surface implants: the background and long-term results, *J. Long Term Eff. Med. Implants*, 9 (3), 247-259 (1999). PMID: 10847966.

[7] J.-C. Schauer, "PECVD-Deposition and Characterization of C-Si Thin Film Systems on Metals", Ph.D. Thesis, Ruhr University, 2007, pp.19-23.

[8] T. Lu, Y.Q. Qiao and X.Y. Liu, Surface modification of biomaterials using plasma immersion ion implantation and deposition, *Interface Focus*, 2, 325–336 (2012). doi: 10.1098/rsfs.2012.0003.

[9] S.J. Bull, "Notes on Surface Engineering" (6 July 2000), Retrieved 20 July 2018, from University of Newcastle: https://www.staff.ncl.ac.uk/s.j.bull/SENotes.html.

[10] H.M. Abourayana, N.A. Zreiba and A.M. Elamin, Synthesis and Characterization of Plasma Polymerized Thin Films Deposited from Benzene and Hexamethyldisiloxane using (PECVD) Method, *International Journal of Chemical, Molecular, Nuclear, Materials and Metallurgical Engineering*, 5 (2), 117-123 (2011).

[11] H.M. Abourayana and D.P. Dowling, "Plasma Processing for Tailoring the Surface Properties of Polymers", in *Surface Energy*, edited by M. Aliofkhazraei, IntechOpen, 2015, pp. 123 -152. doi: 10.5772/60927.

[12] C.S. Wong, R. Mongkolnavin, "Methods of Plasma Generation", in *Elements of Plasma Technology*, Singapore: SpringerNature, 2016, pp. 15-48.

[13] Y.A. Lebedev, "Microwave Discharges: Generation and Diagnostics", in *25th Summer School and International Symposium on the Physics of Ionized Gases – SPIG2010*, edited by L.Č. Popović and M. Kuraica, J. Phys.: Conf. Ser., 257, 012016 (2010). Doi: 10.1088/1742-6596/257/1/012016.

[14] C.A. Destefani, E. Siores and A.B. Murphy, Generation of Microwave-Induced Plasmas in Automotive Exhaust Gas Mixtures Using Pulsed Microwave Energy, *J. Microw. Power Electromagn. Energy*, 38 (2), 95-101 (2003). doi: 10.1080/08327823.2003.11688491.
[15] J.R. Davis, "Overview of biomaterials and their use in medical devices" and "Metallic Materials", in *Handbook of Materials for Medical Devices*, edited by J.R. Davis, Materials Park Ohio: ASM International, 2003, pp. 1-11 & 21-50.
[16] F.J. Baldenebro-Lopez, C.D. Gomez-Esparza, R. Corral-Higuera, S.P. Arredondo-Rea, M.J. Pellegrini-Cervantes, J.E. Ledezma-Sillas, R. Martinez-Sanchez and J.M. Herrera-Ramirez, Influence of Size on the Microstructure and Mechanical Properties of an AISI 304L Stainless Steel—A Comparison between Bulk and Fibers, *Materials*, 8 (2), 451-461 (2015). doi: *10.3390/ma8020451*.
[17] Supporting notes, Surface Modification of Biomaterials, Lecture 9, 3.051J/20.340J, Materials for Biomedical Applications, Spring (2006). https://ocw.mit.edu/courses/materials-science-and-engineering/3-051j-materials-for-biomedical-applications-spring-2006/lecture-notes/lecture 9_2.pdf
[18] A.E. Lefohn, N.M. Mackie and E.R. Fisher, Comparison of Films Deposited from Pulsed and Continuous Wave Acetonitrile and Acrylonitrile Plasmas, *Plasmas Polym.*, 3 (4), 197-209 (1998). doi: *10.1023/A:1021850604696*.
[19] H.G. Kim, S.H. Ahn, J.G. Kim, S.J. Park and K.R. Lee, Electrochemical behavior of diamond-like carbon films for biomedical applications, *Thin Solid Films*, 475, 291-297 (2005). doi: *10.1016/j.tsf.2004.07.052*.
[20] H.G. Kim, S.H. Ahn, J.G. Kim, S.J. Park and K.R. Lee, Corrosion performance of diamond-like carbon (DLC)-coated Ti alloy in the simulated body fluid environment, *Diamond Relat. Mater.*, 14 (1), 35-41 (2005). doi: *10.1016/j.diamond.2004.06.034*.
[21] P. Qi, Y. Yang, S. Zhao, J. Wang, X. Li, Q. Tu, Z. Yang and N. Huang, Improvement of corrosion resistance and biocompatibility of biodegradable metallic vascular stent via plasma allylamine polymerized coating, Mater. Des., 96, 341-349 (2016). doi: 10.1016/j.matdes.2016.02.039.
[22] J. Friedrich, "Plasma Polymerization Mechanism", Federal Institute for Materials Research and Testing, 12200 Berlin, Germany, (2011). Retrieved from *http://home.uni-leipzig.de/iom/muehlleithen/2011/Friedrich_2011.pdf* on 20 July 2018.
[23] A.T. Bell, "The Mechanism and kinetics of plasma polymerization", in *Plasma Chemistry III*, *Topics in Current Chemistry, vol. 94*, edited by S. Vepřek and M. Venugopalan, Berlin Heidelberg: Springer-Verlag, 1980, pp. 43-68. doi: *10.1007/BFb0048586*.
[24] P.H. Li and P.K. Chu; "Thin film deposition technologies and processing of biomaterials"; in Thin Film Coatings for Biomaterials and Biomedical Applications, edited by Hans J Griesser,2016, Pages 3-28, https://doi.org/10.1016/B978-1-78242-453-6.00001-8
[25] B.D. Mistry, *A Handbook of Spectroscopic Data Chemistry (UV, IR, PMR, ^{13}CNMR and Mass Spectroscopy)*, Jaipur India: Oxford Book Company, 2009, pp. 34-45.
[26] Carl Clegg;"Contact Angle Made Easy", 1st edition, USA, (2013), ISBN: *978-1-300-66298-3*
[27] Iqbal, M., Dinh, D. K., Abbas, Q., Imran, M., Sattar, H., & Ahmad, A. U. Controlled surface wettability by plasma polymer surface modification. *Surfaces, (2019), 2*(2), 349–371. https://doi.org/10.3390/surfaces2020026
